

Tunable self-assembled spin chains of strongly interacting cold atoms for demonstration of reliable quantum state transfer

N J S Loft¹, O V Marchukov¹, D Petrosyan², and N T Zinner¹

¹ Department of Physics and Astronomy, Aarhus University, DK-8000 Aarhus C, Denmark

² Institute of Electronic Structure and Laser, FORTH, GR-71110 Heraklion, Crete, Greece

Abstract. We have developed an efficient computational method to treat long, one-dimensional systems of strongly-interacting atoms forming self-assembled spin chains. Such systems can be used to realize many spin chain model Hamiltonians tunable by the external confining potential. As a concrete demonstration, we consider quantum state transfer in a Heisenberg spin chain and we show how to determine the confining potential in order to obtain nearly-perfect state transfer.

PACS numbers: 67.85.-d, 75.10.Pq, 03.67.Lx

Keywords: cold atoms, spin chains, one dimensional physics, strong interactions, quantum state transfer

Submitted to: *New J. Phys.*

1. Introduction

Recent experimental progress with cold atomic gases has opened the door for realizing quantum many-body systems and simulating some of the most useful models of many-body physics [1, 2, 3, 4, 5]. Over the last decade, it has become possible to perform experiments with effective one-dimensional few- and many-body systems [6, 7, 8, 9, 10, 11, 12, 13, 14, 15, 16, 17]. Using Feshbach resonances [18], one can achieve tunable interactions in one-dimensional traps [19] and reach the regime of strongly interacting particles. Combining optical and magnetic traps and standing-wave optical lattices, one may realize different spin models with cold atoms [20, 21] and thus study the static properties and non-equilibrium dynamics of quantum magnetism [22, 23]. In particular, one can realize the paradigmatic Heisenberg spin chain using cold atoms with strong interactions [23].

The local exchange coefficients entering the effective Heisenberg spin chain model are strongly dependent on the geometry of the atom trap. Computing the relation between the trap parameters and the exchange coefficients would provide the essential link between theory and experiment for specific implementations of numerous theoretical spin chain models with strongly interacting cold atomic gases. A method that provides such a link was developed [24, 25], but the computation of the nearest-neighbor interaction coefficients for a system of more than a few atoms was a daunting task. Recently, these computational difficulties were overcome [26, 27, 28] and we can now efficiently treat long one-dimensional systems and obtain self-assembled spin chain Hamiltonians tunable by the external trap potential. Engineering the spin chains in this way allows us to study the delicate interplay between the strong atom-atom interactions and the trap parameters, gaining important theoretical insight into the physics of the experiment.

As a demonstration of our method [26], we will focus here on a specific yet important problem of excitation transfer in spin chains. Within the field of quantum information, a key subject is the study of coherent state and excitation transfer properties of quantum systems [29, 30]. Typically, a quantum computation system is assembled from a number of smaller two-level systems (qubits) interacting with each other and/or with the surrounding environment. Quantum information can be encoded locally by, for instance, preparing an appropriate superposition of spin-up and spin-down states of one of the qubits. As time evolves, this information will propagate through the system and can potentially be retrieved somewhere else. The ability to transfer such quantum information reliably from one point to another is of great importance in quantum information theory. The pioneering work of Bose [31] showed that spin chains are promising candidates for realizing a “quantum bus” that can implement this quantum information transfer.

In 2004 it was shown that one could obtain perfect state transfer in a one-dimensional N -particle spin chain by appropriately tuning the local exchange coefficients [32, 33, 34]. To the best of our knowledge, so far the perfect state transfer protocol was experimentally demonstrated only in the system of evanescently coupled optical waveguides [35, 36]. This is in fact a classical system that can emulate only single particle (non-interacting)

quantum physics, since the coupled-mode equations for a waveguide array are equivalent to the amplitude equations for the single particle (excitation) dynamics in a lattice (chain). It is therefore important to propose and analyze a real many-body quantum system for realizing properly engineered spin chains.

In this paper, we consider a cold-atom implementation of such a system. We demonstrate our efficient computation method by investigating how the trap potential can be chosen in order to obtain perfect state transfer for up to $N = 20$ particles. Furthermore, we consider how sensitive is the state transfer to the experimentally realistic noise. The noise in our calculations is included exactly in the sense that we add fluctuations to the external potential and then compute the local exchange coefficients. This should be contrasted with first approximating the true continuum Hamiltonian by a lattice model in the strongly interacting limit, and then adding homogeneous noise to the coefficients of the lattice model. Here we abstain from the approximate lattice description and include the noise already in the continuum model from which we compute the corresponding spin chain parameters and their uncertainties. We find that high-fidelity state transfer can tolerate moderate amount of noise, thus suggesting that the cold-atom implementations of truly many-body quantum systems for quantum information applications are well-suited for experimental study.

The paper is organized as follows: In Section 2 we briefly explain how the strongly interacting cold-atom gas is related to the spin chain system and sketch the solution for this general problem. In Section 3 we introduce the particular spin chain system exhibiting perfect state transfer properties, and we find the nearly optimal form of the confining potential for the cold-atom gas. In Section 4 we study experimentally realistic fluctuations of the trapping potential and show that the transfer is tolerant to a moderate amount of the resulting noise. We close the paper by summarizing our results.

2. The general spin chain problem

We begin with an outline of the general spin chain problem and its connection to strongly interacting one-dimensional gases, summarizing some important results from Ref. [37] (for related studies that also map the strongly-interacting systems onto spin models see Refs. [25, 28, 38, 39, 40, 41]). The general problem concerns N strongly-interacting particles with mass m in an arbitrary one-dimensional confining potential $V(x)$. We consider two species (spin states) of particles, denoting by N_{\uparrow} the number of spin-up particles and by $N_{\downarrow} = N - N_{\uparrow}$ the number of spin-down particles. Particles of different species interact via a contact potential with strength $g > 0$ and of the same species with strength κg with $\kappa > 0$. The Hamiltonian of the system is

$$\begin{aligned}
 H = \sum_{i=1}^N \left[-\frac{\hbar^2}{2m} \frac{\partial^2}{\partial x_i^2} + V(x_i) \right] + g \sum_{\uparrow\downarrow} \delta(x_i - x_j) \\
 + \kappa g \sum_{\uparrow\uparrow} \delta(x_i - x_j) + \kappa g \sum_{\downarrow\downarrow} \delta(x_i - x_j), \tag{1}
 \end{aligned}$$

where the sum over $\uparrow\downarrow$ is understood as a sum over the $N_\uparrow \cdot N_\downarrow$ pairs of particles of different species, while the sum over $\uparrow\uparrow$ is over all $N_\uparrow \cdot (N_\uparrow - 1)/2$ pairs of spin-up particles, and similarly for $\downarrow\downarrow$. As noted in Ref. [37], the Hamiltonian of Eq. (1) is valid for both bosons and fermions.

For strong interaction $g \gg 1$ and $\kappa \gg 1/g$, we can solve for the system described by Eq. (1) exactly, to first order in $1/g$, if we know the N lowest-energy eigenstates of the single-particle Hamiltonian

$$H_1(x) = -\frac{\hbar^2}{2m} \frac{\partial^2}{\partial x^2} + V(x). \quad (2)$$

If the trap potential $V(x)$ is sufficiently well-behaved, solving the Schrödinger equation $H_1\psi_i = E_i\psi_i$ numerically is an elementary exercise. Since we are interested in strong interactions, we perturb the system away from the Tonks-Girardeau (TG) limit $1/g \rightarrow 0$. In this limit, the ground state is $N!/(N_\uparrow! \cdot N_\downarrow!)$ -fold degenerate. We denote this TG ground state energy by E_0 , which is also the energy of the (non-normalized) Slater determinant wave function $\Phi_0(x_1, \dots, x_N)$ composed of the N single-particle eigenfunctions $\psi_i(x)$. From now on we will use the units of $\hbar = m = 1$.

Moving slightly away from the TG limit, the ground-state degeneracy is lifted, and the Hamiltonian can be mapped onto a Heisenberg spin chain model. To linear order in $1/g \ll 1$, the Hamiltonian can be written as

$$H = E_0 - \sum_{k=1}^{N-1} \frac{\alpha_k}{g} \left[\frac{1}{2} (1 - \boldsymbol{\sigma}^k \cdot \boldsymbol{\sigma}^{k+1}) + \frac{1}{\kappa} (1 + \sigma_z^k \sigma_z^{k+1}) \right], \quad (3)$$

where $\boldsymbol{\sigma}^k = (\sigma_x^k, \sigma_y^k, \sigma_z^k)$ are the Pauli matrices acting on the spin of the particle at k th position, and α_k are the coefficients determined solely by the trapping potential $V(x)$ [37]. In other words, the geometric coefficients α_k only depend on the *geometry* of the trap. Calculation of all the geometric coefficients for a given trap potential would determine the spin chain model in Eq. (3) equivalent to the system of trapped, strongly-interacting particles in Eq. (1).

Volosniev *et al.* [37] have derived the following expression for the geometric coefficients,

$$\alpha_k = \int_{x_1 < x_2 < \dots < x_{N-1}} dx_1 dx_2 \dots dx_{N-1} \left(\frac{\partial \Phi_0(x_1, \dots, x_N)}{\partial x_N} \right)_{x_N=x_k}^2. \quad (4)$$

If we are interested in more than just a few particles, it quickly becomes impossible to numerically evaluate the $N - 1$ integrals of Eq. (4) accurately. Thus, in order to calculate the geometric coefficients α_k for many-particle systems, the above expression should be rewritten in a form that is better suited for numerical implementation. Such an expression was derived in Ref. [26]:

$$\alpha_k = \sum_{i=1}^N \left[\frac{d\psi_i}{dx} \right]_{x=b}^2 + 2 \sum_{i=1}^N \sum_{j=1}^N \sum_{l=0}^{N-1-k} \frac{(-1)^{i+j+N-k}}{l!} \binom{N-l-2}{k-1} \times \int_a^b dx \frac{2m}{\hbar^2} (V(x) - E_i) \psi_i(x) \frac{d\psi_j}{dx} \left[\frac{\partial^l}{\partial \lambda^l} \det [(B(x) - \lambda \mathbf{I})^{(ij)}] \right]_{\lambda=0}, \quad (5)$$

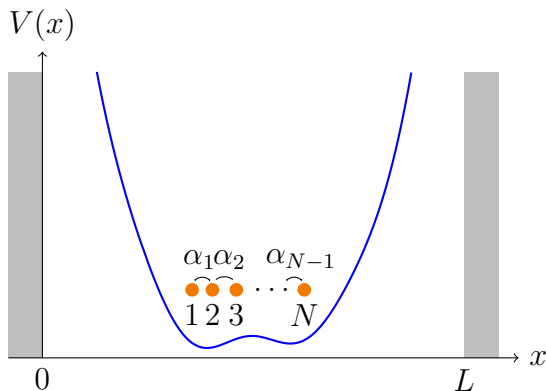


Figure 1. Sketch of an N particle spin chain in a trapping potential $V(x)$. We are able to calculate the spin-exchange coefficients α_k governing the dynamics of the system for any potential and $N \lesssim 35$. In our numerical implementation, the system is placed in a hard-wall box ranging from $x = 0$ to $x = L$. This restricts the system to a finite region of space, but the length L can be chosen so large that the cut-off does not affect the N lowest-energy single-particle states in the trap potential $V(x)$ and hence the corresponding α_k coefficients.

where $B(x)$ is an $N \times N$ symmetric matrix constructed from ψ_i , $i = 1, \dots, N$, with mn 'th entry given by $\int_a^x dy \psi_m(y) \psi_n(y)$, and $(\)^{(ij)}$ denotes a minor obtained by removing the i 'th column and the j 'th row, while $[a; b]$ is the spatial interval containing the system. Despite its complicated appearance, Eq. (5) is amenable to efficient numerical implementation, as detailed in Ref. [26], where we also present a well-working numerical code in C freely available to anyone. In our program, we place the system in a box with impenetrable hard walls in order to fully confine it to a finite region of space $[a; b] = [0; L]$, see Figure 1. The length of the box, L , can always be chosen sufficiently large so as not to affect the N lowest-energy single-particle states in the trapping potential $V(x)$ that are needed to compute the expression in Eq. (5). The wavefunctions $\psi_i(x)$ are expanded in terms of the standing-wave sinusoidal eigenfunctions for the box potential. Our program was first used in Ref. [27] to calculate the geometric coefficients for $N \leq 30$ particles in the special case of a harmonic trap potential. The calculation for $N = 30$ was accomplished in a matter of hours on a small personal computer, while reliable results could be easily obtained for even more particles. The program can handle arbitrary potentials, which we exploit in this paper to study the quantum state transfer in engineered spin chains of nontrivial lengths.

3. Perfect state transfer potential

Consider a chain of N interacting spin- $\frac{1}{2}$ fermions described by the Heisenberg XXZ model Hamiltonian

$$H_{\text{SC}} = -\frac{1}{2} \sum_{k=1}^{N-1} J_k (\sigma_x^k \sigma_x^{k+1} + \sigma_y^k \sigma_y^{k+1} + \Delta \sigma_z^k \sigma_z^{k+1}) , \quad (6)$$

where $J_k = -\alpha_k/g$ are the nearest-neighbor interaction coefficients, and Δ is the asymmetry parameter, which is related to the interaction parameter κ via $\Delta = (1 - 2/\kappa)$. In the following, we consider the Heisenberg XX model, i.e. we assume $\Delta = 0$ or $\kappa = 2$. Notice that H_{SC} conserves the total spin projection $(N_{\uparrow} - N_{\downarrow})/2$. Suppose that the initial state of the system at time $t = 0$ is $|1\rangle \equiv |\uparrow\downarrow\downarrow \cdots \downarrow\downarrow\rangle$, meaning that the particle at site 1 is in the spin-up state while the remaining $N - 1$ particles are spin-down. In general, this state is not an eigenstate of the system, so the initial state will evolve with time into a linear combination of states with exactly one spin-up particle somewhere in the chain. We are interested in whether the spin-up state is transferred to site N at the opposite end of the chain, i.e. the system ends up in state $|N\rangle \equiv |\downarrow\downarrow\downarrow \cdots \downarrow\uparrow\rangle$. The time dependent probability of successful spin transfer is

$$F(t) = |\langle N | e^{-iH_{\text{SC}}t/\hbar} | 1 \rangle|^2 . \quad (7)$$

This quantity is known as the fidelity, and $F(t) = 1$ would correspond to perfect transfer at time t .

It was shown in Refs. [32, 33, 34] that one can obtain perfect state or excitation transfer if the nearest-neighbor exchange coefficients $J_k \propto \alpha_k$ follow the form

$$\alpha_k \propto \sqrt{k(N - k)} , \quad (8)$$

corresponding to a semicircular shape. Remarkably, the optimal (fastest) and perfect state transfer is obtained for any number N of particles in the chain [42]. The pertinent question now is how to experimentally realize the system such that the interaction coefficients have the correct form. With a cold-atom implementation of the spin chain, this question reduces to that of choosing a trapping potential $V(x)$ of proper shape, which is what we investigate below.

3.1. Connection between $V(x)$ and the α_k 's

Our goal is to determine the shape of the trapping potential $V(x)$ which results in the geometric coefficients following the distribution of Eq. (8) for an N -particle spin chain. With the length scale of the potential ℓ , the corresponding energy scale is $\epsilon = \hbar^2/(2m\ell^2)$. In our numerical program, we place the system into a hard-wall box of large size $L = 100\ell$.

Before describing a class of candidate potentials, we present a useful observation concerning the relation between the shapes of $V(x)$ and α_k 's. The geometric coefficients of Eq. (4) only depend on $V(x)$ through the Slater determinant wavefunction, Φ_0 , composed of the eigenstates of the single-particle Hamiltonian (2). Even though we start with a simple function $V(x)$ and end up with a set of $N - 1$ numbers α_k , the precise relation between the two is still extremely complicated. However, as is evident from Figure 2, the geometric coefficients approximately follow the shape of $-V(x)$. An intuitive explanation is that the deeper is the potential, the more is the overlap of the spatial wavefunctions of neighboring particles, and therefore the larger is the corresponding geometric coefficient describing the spin-exchange amplitude. This seems

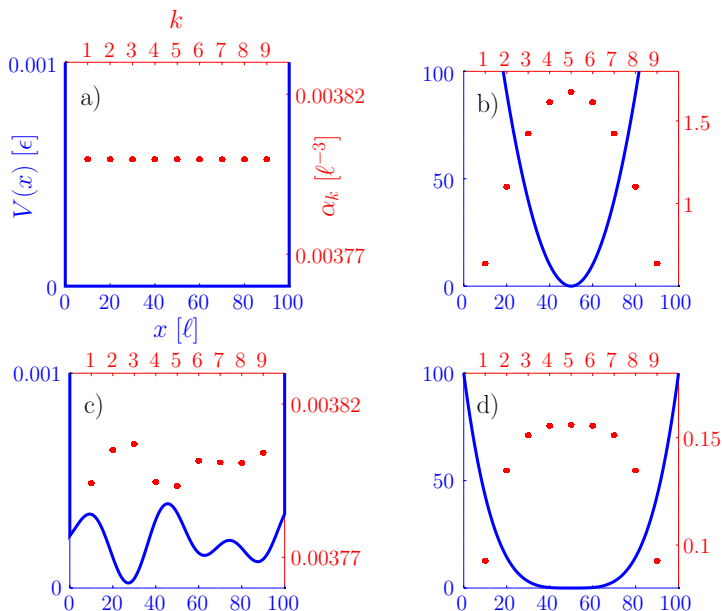


Figure 2. The amplitudes of geometric coefficients approximately follow the shape of $-V(x)$. For $N = 10$ particles, we show the potential $V(x)$ (blue line) and the geometric coefficients α_k (red dots) for (a) hard wall potential, (b) harmonic potential, (c) hard wall potential with noise and (d) our optimized state transfer potential of Eq. (9) with $\tau = 3.793287$. The units are indicated on the corresponding axes of (a).

to imply that a local density approximation should work well in some cases. For a detailed study of this question we refer the reader to Ref. [43].

This observation motivates us to choose a trial trapping potential which resembles the shape of semicircle. We choose the simple “bowl-shaped” potential (see Figure 2(d)).

$$V(x) = 100\epsilon \cdot \left| \frac{L/2 - x}{L/2} \right|^\tau, \quad (9)$$

where τ is an adjustable parameter. The scale factor of 100 is set large enough to ensure that the hard-wall boundaries do not affect the N lowest-energy single-particle states in $V(x)$ and thereby the calculation of the geometric coefficients ‡. The idea now is quite simple: For any given N , we calculate the set of geometric coefficients corresponding to the potential in Eq. (9) for some τ . We then fit the produced $N - 1$ geometric coefficients to a function of the form

$$\alpha_k \propto [k(N - k)]^\beta, \quad (10)$$

where β is a fit parameter such that the desired semicircle distribution of Eq. (8) corresponds to $\beta = 1/2$. If we can find a value of τ for which $\beta = 1/2$, and if the fit is good, we expect the system to exhibit perfect state transfer. Since the trial potential

‡ Notice that $V(0) = V(L) = 100\epsilon$, whereas the highest single-particle state we use has much smaller energy of 7.80ϵ (the energy of the 20th state for $N = 20$), so the hard wall boundaries do not influence the calculation of the geometric coefficients.

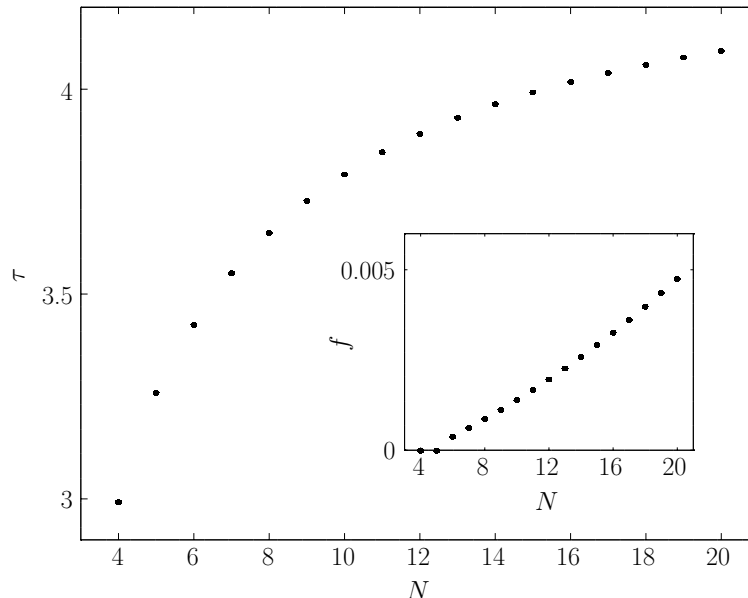


Figure 3. For the τ -dependent trial potential (9) we fit the corresponding geometric coefficients to Eq. (10). The main panel shows values of τ optimized to produce the fit parameter $\beta = 1/2$ for different particle numbers N . The inset shows the corresponding goodness of the fit f .

of Eq. (9) is rather simple, with only one adjustable parameter, we do not in general expect to be able to obtain a perfect fit of the geometric coefficients. Optimizing τ such that the best fit produces $\beta = 1/2$ yields the results of Figure 3, where we also show a measure for the goodness of the fit f . It is not surprising that the fit is better for smaller N because the number of fit points is $N - 1$. The geometric coefficients corresponding to the optimized potential are given in Appendix A.

3.2. Perfect state transfer

To check whether the optimized potentials lead to perfect state transfer, we calculate the fidelity of Eq. (7). In the Heisenberg XX spin chain with coupling constants given by $J_k \propto -\alpha_k \propto -\sqrt{k(N-k)}$, the optimal transfer time is $t_0 = \hbar\pi\sqrt{N-1}/2|J_1|$ [32, 33, 42]. In Figure 4 we observe that the fidelity at $t = t_0$ does indeed indicate a nearly-perfect transfer for the smaller values of N we consider, but then $F(t_0)$ quickly decreases for $N \geq 10$. Generally, the maximum of $F(t)$ occurs at a time t_{out} slightly before t_0 , see the inset of Figure 4. We may think of t_{out} as the retrieval (or measurement) time, and we obtain good transfer fidelity $F(t_{\text{out}}) \geq 0.95$ for all $N \leq 20$. Next, we will study how the fidelity is affected by noise stemming from fluctuations of the potential.

§ Let (y_i, x_i) be the data points for $i = 1, \dots, n$ we wish to fit to the model function $y(x)$. We define the goodness of the fit as the length of the vector of differences $f_i = y(x_i) - y_i$ normalized by the number of data points, $f = \frac{1}{n} \sqrt{\sum_{i=1}^n f_i^2}$; clearly smaller f corresponds to better fit.

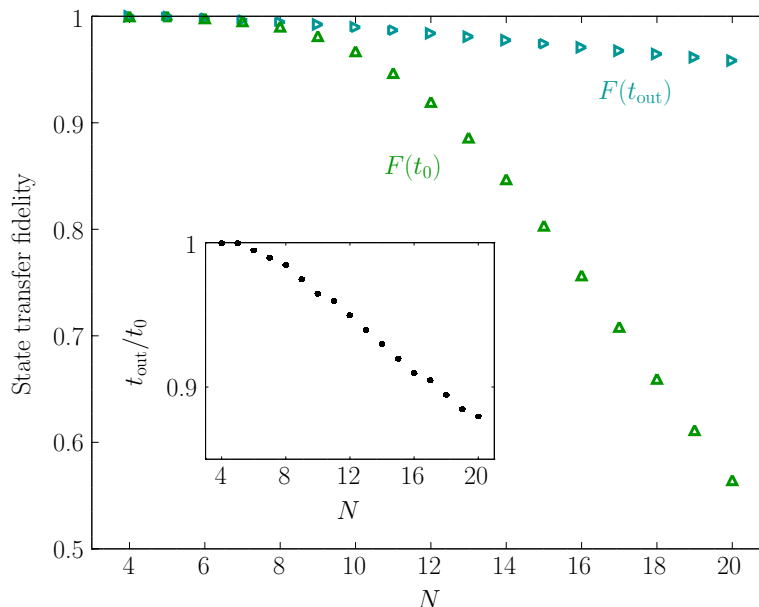


Figure 4. The main panel shows the transfer fidelity F at times t_0 and t_{out} for different N . The inset shows the corresponding ratio t_{out}/t_0 .

4. Noise tolerant state transfer

In the previous section, we saw that the atoms in a trapping potential of the form of Eq. (9) form a self-assembled spin chain which can mediate nearly-perfect state transfer between its two ends. Our theoretical calculations so far assumed idealized situation in which the potential is well-defined and engineered to maximize the transfer fidelity. In any real experiment, however, there will be uncontrollable fluctuations of the potential. In this section we study how the resulting noise will influence the retrieval fidelity $F(t_{\text{out}})$. We emphasize that we consider uncontrolled variations of the potential leading to a noisy spin chain. In other words, we treat the noise exactly by including it in the original system, before we derive an effective spin chain parameters. This is in contrast to the usual approach [44, 45, 46, 47], in which one typically includes uniform, Gaussian or colored noise in the interaction parameters of the spin lattice model, without specifying the original source of the fluctuations.

4.1. Random noise on the potential

We add a noise term $\delta V(x)$ to the optimized potential $V(x)$ of Eq. (9) in the form of a quasi-periodic potential [48]:

$$\delta V(x) = V_0 [\cos(x/\ell + \phi_1) + \cos(\xi x/\ell + \phi_2)] , \quad (11)$$

where V_0 is the strength of the noise, $\phi_1, \phi_2 \in [0; 2\pi[$ are uniformly distributed random phases, and ξ is an irrational number chosen to be $\xi = 2/(1 + \sqrt{5}) \approx 0.618$.

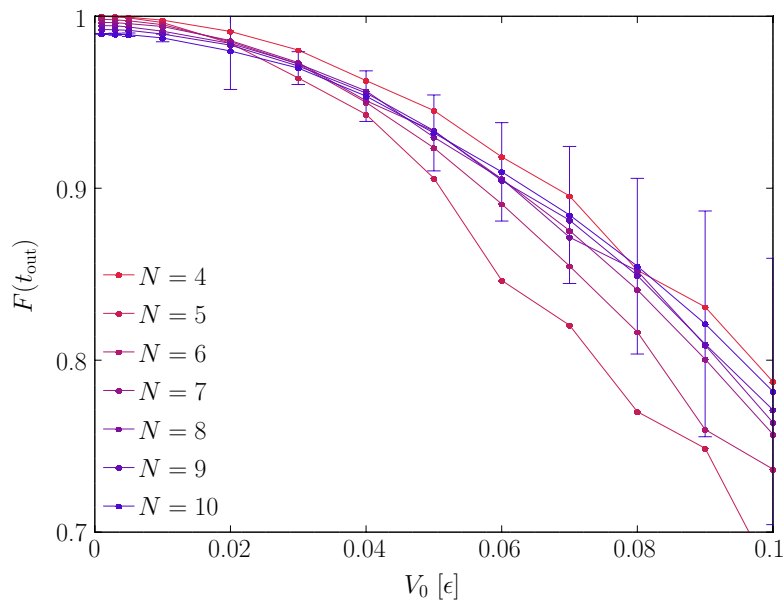


Figure 5. Retrieval fidelity, $F(t_{\text{out}})$, as a function of noise strength V_0 , for different particle numbers N . The error bars for $N = 10$ are one standard deviation. The standard deviations for other values of N are similar, but not shown for better readability.

To quantify how $F(t_{\text{out}})$, for a given number of particles $N \leq 10$, is affected by the noise of Eq. (11), we take an ensemble of $M = 200$ random phases ϕ_1 and ϕ_2 for each noise strength V_0 and calculate the corresponding M sets of geometric coefficients. The resulting average fidelities $F(t_{\text{out}})$ and their uncertainties (for the case of $N = 10$) are shown in Figure 5. The noise strength V_0 should be compared to the typical energy scale of the system ϵ ||. We thus verify that the state transfer can tolerate uncontrolled variations of the trapping potential at a few percent level, $V_0 < 0.02\epsilon$. We estimate that for a potential $V(x)$ with a typical length scale ℓ of several microns, the energy scale $\epsilon \approx 500$ Hz. This then leads to $V_0 < 10$ Hz, which is experimentally realistic but not trivial.

In Figure 5 we observe that for a weak noise the fidelity is larger for smaller particle numbers N , which is consistent with our observation above that in the noise-free limit $F(t_{\text{out}})$ slowly decreases with increasing N . With increasing the noise strengths, however, the fidelity generally decreases faster for smaller values of N (except for $N = 4$), which means that longer chains are more robust. A probable reason for this behavior is averaging out of the potential fluctuations which is perhaps more complete for larger systems.

It is instructive to quantify the response of the exchange coefficients to the fluctuations of the potential. For a fixed value of the noise strength V_0 , we denote

|| For $N = 4, \dots, 10$, the energy of the N 'th single-particle state ranges from 0.55ϵ to 1.21ϵ , which characterizes the energy scale of the system.

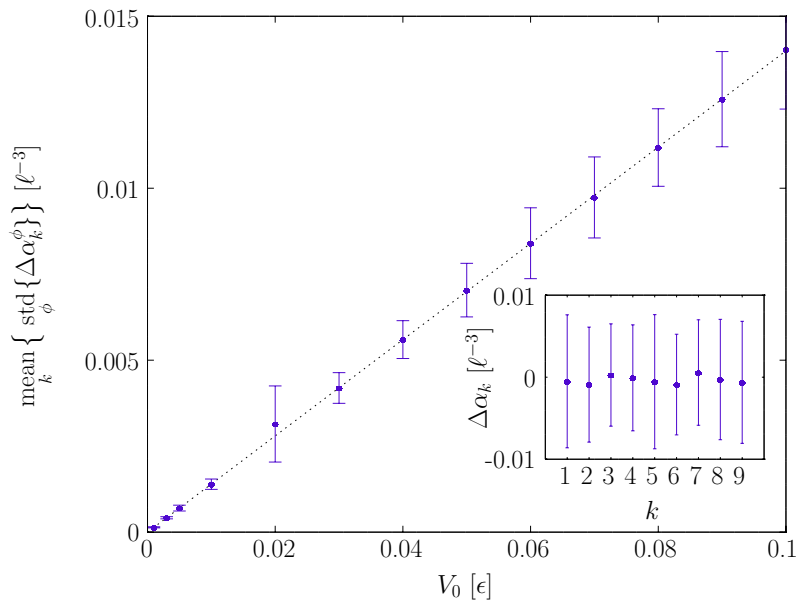


Figure 6. Fluctuating potential produces noise on the geometric coefficients α_k . The results are obtained for the $N = 10$ -particle system with $M = 200$ realizations of the fluctuating potential for each value of the noise strength V_0 . The main panel shows the uncertainties (one standard deviation) of $\Delta\alpha_k$, averaged over all $k = 1, \dots, 9$, versus V_0 . A fit to the data yields the proportionality factor of $(0.13994 \pm 0.00427)\ell^{-3}\epsilon^{-1}$. The inset shown $\Delta\alpha_k$'s for $V_0 = 0.05\epsilon$, with error bars corresponding to one standard deviation.

by α_k^ϕ the k 'th coefficient for a given realization of the noisy potential with two particular values for the random phases ϕ_1 and ϕ_2 . The deviation from the noise-free coefficient α_k recorded in Appendix A is denoted by $\Delta\alpha_k^\phi \equiv \alpha_k - \alpha_k^\phi$. Similarly to the random noise introduced directly into the coefficients [44, 45], the deviations $\Delta\alpha_k^\phi$ averaged over many ($M = 200$) realizations of the noisy potential, $\Delta\alpha_k \equiv \text{mean}_\phi \{ \Delta\alpha_k^\phi \}$, are approximately zero for all k . In the inset of Figure 6 we show the mean deviations $\Delta\alpha_k$ and their uncertainties, $\text{std}_\phi \{ \Delta\alpha_k^\phi \}$, for the case of $V_0 = 0.05\epsilon$. Since the uncertainties are approximately equal for all k , we average the uncertainties over all k and plot the result versus the noise strength V_0 in Figure 6 main panel. The data follow a proportionality law with a slope equal to $(0.13994 \pm 0.00427)\ell^{-3}\epsilon^{-1}$. This simple relation can indeed be useful as it provides direct link between the experimental uncertainties and noise on the coefficients appearing in the effective spin model.

4.2. Tilting the potential

The second kind of experimental uncertainty we consider is tilting the potential by adding a parity breaking linear term:

$$\delta V(x) = V_0 [x - L/2]/\ell, \quad (12)$$

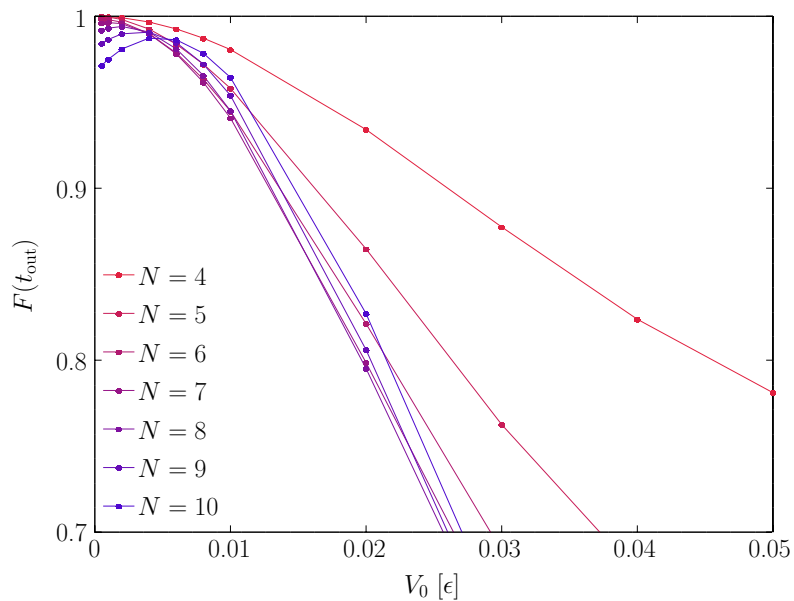


Figure 7. Retrieval fidelity for $N = 10$ particles in a tilted potential as a function of tilt amplitude V_0 which should be compared to the typical energy scale of 0.03ϵ .

where V_0 is a parameter for the tilt amplitude with units of energy. The value of the slope V_0/ℓ should be compared to the typical energy-over-length scale of the system. An estimate for this scale for $N = 10$ is the quotient between the energy and the spatial extent of the wavefunction for the 10th single-particle state, which is $1.21\epsilon/(40\ell) = 0.03\epsilon/\ell$. In Figure 7 we show the state transfer fidelity resulting from adding the tilt term of Eq. (12) to the optimized potential. We find that the system is tolerant to weak to moderate tilting noise, $V_0 < 0.005\epsilon$ (for $N \sim 10$, a sufficiently small tilt even improves the transfer). Larger tilts would strongly suppress state transfer.

5. Summary

To conclude, we have employed our efficient computational method to study the possibility of realizing self-assembled spin chain systems with strongly-interacting cold atomic gases in one-dimensional trapping potentials. The parameters of the effective spin chains are tunable by the confining potential, which can serve as a valuable experimental tool.

As an important concrete example of quantum dynamics in a many-body system, we considered quantum state transfer in the effective spin chains of cold atoms. We demonstrated how the confining potential could be tuned to achieve nearly-perfect transfer of a spin excitation between the two ends of the chain. To emphasize the experimental feasibility of our proposal, we showed that the cold-atom implementation of a spin chain is tolerant to moderate noise. Importantly, we considered noise rigorously by including it directly in the potential, and not at the level of the effective lattice Hamiltonian which is only an approximate way of including noise.

In closing we note that throughout this study we have assumed zero temperature gas of N strongly-interacting atoms occupying the N lowest-energy single-particle eigenstates of the trapping potential. This approximation is valid for temperatures $k_B T \ll \epsilon$, where k_B is the Boltzmann constant while ϵ is the typical energy scale of the potential which characterizes the particle excitation energies. If this condition is not satisfied, we would have to consider a thermal distribution of occupation probabilities of different excitation manifolds of N atoms. For each such manifold, we can construct a Slater determinant wavefunction and the corresponding spin chain model [37], which in general will have different local exchange coefficients. Hence, the spin dynamics will experience decoherence, the more so the higher is the temperature and the larger is the number of excited energy manifolds with non-negligible population. We leave further details for future studies.

Acknowledgments The authors wish to thank A. G. Volosniev, M. Valiente and J. M. Midtgaard for helpful discussions and comments during the preparation of the manuscript. We are grateful to L. B. Kristensen and A. E. Thomsen for development of the computational methods to determine the geometric coefficients. This work was supported by the Carlsberg Foundation and by the Danish Council for Independent Research DFF Natural Sciences and the DFF Sapere Aude program.

Appendix A. Geometric coefficients for the state transfer optimized potential

In Section 3 we optimized the τ -dependent potential of Eq. (9) such that the geometric coefficients followed, as close as possible, a semicircle distribution, leading to perfect state transfer in the spin chain. Here we record the optimized values of τ and the corresponding $N - 1$ geometric coefficients. Since the potential is symmetric, the coefficients have the property $\alpha_k = \alpha_{N-k}$, and we only show the values of half of them, continuing on the next line as necessary.

N	τ	α_1	α_2	α_3	...						
4	2.993540	0.0475251	0.0548772								
5	3.260198	0.0510611	0.0625369								
6	3.426142	0.0579675	0.0745497	0.0766875							
7	3.552248	0.0658202	0.0880452	0.0926727							
8	3.650098	0.0743862	0.1027688	0.1106852	0.1116192						
9	3.728815	0.0834554	0.1184395	0.1303163	0.1326455						
10	3.793287	0.0929392	0.1349339	0.1513421	0.1557556	0.1562500					
11	3.847014	0.1027691	0.1521459	0.1735853	0.1807227	0.1820661					
12	3.892360	0.1128996	0.1700001	0.1969183	0.2073502	0.2100762	0.2103721				
13	3.931069	0.1232943	0.1884324	0.2212349	0.2354734	0.2401236	0.2409746				
14	3.964425	0.1339250	0.2073901	0.2464477	0.2649561	0.2720442	0.2738566	0.2740494			
15	3.993409	0.1447681	0.2268279	0.2724815	0.2956824	0.3056874	0.3089038	0.3094809			
16	4.018780	0.1558040	0.2467065	0.2992711	0.3275525	0.3409190	0.3459820	0.3472557	0.3473895		
17	4.041134	0.1670160	0.2669916	0.3267593	0.3604793	0.3776203	0.3849582	0.3872880	0.3877002		
18	4.060946	0.1783897	0.2876529	0.3548955	0.3943860	0.4156856	0.4257072	0.4294682	0.4304027	0.4305001	
19	4.078598	0.1899124	0.3086636	0.3836347	0.4292043	0.4550208	0.4681135	0.4736811	0.4754314	0.4757379	
20	4.094403	0.2015732	0.3299996	0.4129363	0.4648732	0.4955414	0.5120715	0.5198130	0.5226962	0.5234059	0.5234795

- [1] M. Lewenstein, A. Sanpera, V. Ahufinger, B. Damski, A. Sen(De), and U. Sen. Ultracold atomic gases in optical lattices: mimicking condensed matter physics and beyond. *Advances in Physics*, 56(2):243–379, 2007.
- [2] I. Bloch, J. Dalibard, and W. Zwerger. Many-body physics with ultracold gases. *Rev. Mod. Phys.*, 80:885–964, 2008.
- [3] T. Esslinger. Fermi-Hubbard physics with atoms in an optical lattice. *Annual Review of Condensed Matter Physics*, 1(1):129–152, 2010.
- [4] M. A. Baranov, M. Dalmonte, G. Pupillo, and P. Zoller. Condensed Matter Theory of Dipolar Quantum Gases. *Chem. Rev.*, 112(9):5012–5061, 2012.
- [5] N. T. Zinner and A. S. Jensen, Comparing and contrasting nuclei and cold atomic gases. *Journal of Physics G: Nuclear and Particle Physics*, 40(5):053101, 2013.
- [6] H. Moritz, T. Stöferle, M. Köhl, and T. Esslinger. Exciting Collective Oscillations in a Trapped 1D Gas. *Phys. Rev. Lett.*, 91(25):250402, 2003.
- [7] T. Stöferle, H. Moritz, C. Schori, M. Köhl, and T. Esslinger. Transition from a Strongly Interacting

- 1D Superfluid to a Mott Insulator. *Phys. Rev. Lett.*, 92(13):130403, 2004.
- [8] T. Kinoshita, T. Wenger, and D. S. Weiss. Observation of a One-Dimensional Tonks-Girardeau Gas. *Science*, 305(5687):1125–1128, 2004.
- [9] B. Paredes *et al.*. TonksGirardeau gas of ultracold atoms in an optical lattice. *Nature*, 429:277–281, 2004.
- [10] T. Kinoshita, T. Wenger, and D. S. Weiss. A quantum Newton’s cradle. *Nature*, 440:900–903, 2006.
- [11] E. Haller *et al.*. Realization of an Excited, Strongly Correlated Quantum Gas Phase. *Science*, 325(5945):1224–1227, 2009.
- [12] E. Haller *et al.*. Pinning quantum phase transition for a Luttinger liquid of strongly interacting bosons. *Nature*, 466:597–600, 2010.
- [13] F. Serwane *et al.*. Deterministic Preparation of a Tunable Few-Fermion System. *Science*, 332(6027):336–338, 2011.
- [14] G. Zürn *et al.*. Fermionization of Two Distinguishable Fermions. *Phys. Rev. Lett.*, 108(07):075303, 2012.
- [15] A. Wenz *et al.*. From Few to Many: Observing the Formation of a Fermi Sea One Atom at a Time. *Science*, 342(6157):457–460, 2013.
- [16] G. Pagano *et al.*. A one-dimensional liquid of fermions with tunable spin. *Nature Phys.*, 10:198–201, 2014.
- [17] S. Murmann *et al.*. Two Fermions in a Double Well: Exploring a Fundamental Building Block of the Hubbard Model. *Phys. Rev. Lett.*, 114(08):080402, 2015.
- [18] C. Chin, R. Grimm, P. S. Julienne, E. and Tiesinga. Feshbach resonances in ultracold gases. *Rev. Mod. Phys.*, 82(2):1225, 2010.
- [19] M. Olshanii. Atomic Scattering in the Presence of an External Confinement and a Gas of Impenetrable Bosons. *Phys. Rev. Lett.*, 81(5):938, 1998.
- [20] A. B. Kuklov, B. V. Svistunov. Counterflow Superfluidity of Two-Species Ultracold Atoms in a Commensurate Optical Lattice. *Phys. Rev. Lett.*, 90(10):100401, 2003.
- [21] L.-M. Duan, E. Demler, and M. D. Lukin. Controlling Spin Exchange Interactions of Ultracold Atoms in Optical Lattices. *Phys. Rev. Lett.*, 91(9):090402, 2003.
- [22] T. Fukuhara *et al.*. Quantum dynamics of a mobile spin impurity. *Nature Phys.*, 9:235–241, 2013.
- [23] S. Hild *et al.*. Far-from-Equilibrium Spin Transport in Heisenberg Quantum Magnets. *Phys. Rev. Lett.*, 113(14):147205, 2014.
- [24] A. G. Volosniev, D. V. Fedorov, A. S. Jensen, M. Valiente, and N. T. Zinner. Strongly interacting confined quantum systems in one dimension. *Nature Commun.*, 5:5300, 2014.
- [25] F. Deuretzbacher, D. Becker, J. Bjerlin, S. M. Reimann, and L. Santos. Quantum magnetism without lattices in strongly interacting one-dimensional spinor gases. *Phys. Rev. A*, 90(1):013611, 2014.
- [26] N. J. S. Loft, L. B. Kristensen, A. E. Thomsen, A. G. Volosniev, and N. T. Zinner. CONAN – the cruncher of local exchange coefficients for strongly interacting confined systems in one dimension. *ArXiv e-prints*, arXiv:1603.02662, 2016.
- [27] N. J. S. Loft, L. B. Kristensen, A. E. Thomsen, and N. T. Zinner. Comparing models for the ground state energy of a trapped one-dimensional Fermi gas with a single impurity. *ArXiv e-prints*, arXiv:1508.05917, 2015.
- [28] F. Deuretzbacher, D. Becker, and L. Santos, Momentum distributions and numerical methods for strongly interacting one-dimensional spinor gases. *ArXiv e-prints*, arXiv:1602.06816, 2016
- [29] S. Bose. Quantum Communication through Spin Chain Dynamics: an Introductory Overview. *Contemp. Phys.*, 48(1):13–30, 2007;
D. Burgarth. Quantum state transfer and time-dependent disorder in quantum chains. *Eur. Phys. J. Special Topics*, 151(1):147–155, 2007.
- [30] G. M. Nikolopoulos and I. Jex (eds.). Quantum State Transfer and Network Engineering. Springer, Berlin, 2014.

- [31] S. Bose. Quantum Communication through an Unmodulated Spin Chain. *Phys. Rev. Lett.*, 91(20):207901, 2003.
- [32] M. Christandl, N. Datta, A. Ekert, and A.J. Landahl. Perfect State Transfer in Quantum Spin Networks. *Phys. Rev. Lett.*, 92(18):187902, 2004;
M. Christandl, N. Datta, T.C. Dorlas, A. Ekert, A. Kay and A.J. Landahl, Perfect transfer of arbitrary states in quantum spin networks *Phys. Rev. A*, 71(3):032312, 2005.
- [33] G. M. Nikolopoulos, D. Petrosyan, and P. Lambropoulos. Coherent electron wavepacket propagation and entanglement in array of coupled quantum dots. *Europhys. Lett.*, 65(3):297, 2004;
G. M. Nikolopoulos, D. Petrosyan, and P. Lambropoulos. Electron wavepacket propagation in a chain of coupled quantum dots. *J. Phys.: Condens. Matter*, 16(28):4991, 2004.
- [34] M.B. Plenio, J. Hartley, and J. Eisert. Dynamics and manipulation of entanglement in coupled harmonic systems with many degrees of freedom. *New J. Phys.* 6:36, 2004.
- [35] M. Bellec, G.M. Nikolopoulos and S. Tzortzakis. Faithful communication Hamiltonian in photonic lattices. *Opt. Lett.*, 37(21):4504–4506, 2012.
- [36] A. Perez-Leija, R. Keil, A. Kay, H. Moya-Cessa, S. Nolte, L.-C. Kwek, B. M. Rodriguez-Lara, A. Szameit, and D. N. Christodoulides. Coherent quantum transport in photonic lattices. *Phys. Rev. A*, 87(1):012309, 2013.
- [37] A. G. Volosniev, D. Petrosyan, M. Valiente, D. V. Fedorov, A. S. Jensen, and N. T. Zinner. Engineering the dynamics of effective spin-chain models for strongly interacting atomic gases. *Phys. Rev. A*, 91(2):023620, 2015.
- [38] L. Yang, L. Guan, and H. Pu. Strongly interacting quantum gases in one-dimensional traps. *Phys. Rev. A*, 91(4):043634, 2015.
- [39] J. Levinsen, P. Massignan, G. M. Bruun, and M. M. Parish. Strong-coupling ansatz for the one-dimensional Fermi gas in a harmonic potential. *Science Advances*, 1(6):e1500197, 2015.
- [40] H. Hu, L. Guan, and S. Chen. Strongly interacting Bose-Fermi mixtures in one dimension. *New J. Phys.*, 18:025009, 2016.
- [41] L. Yang and X. Cui. Effective spin-chain model for strongly interacting one-dimensional atomic gases with an arbitrary spin. *Phys. Rev. A*, 93(1):013617, 2016.
- [42] M.-H. Yung. Quantum speed limit for perfect state transfer in one dimension. *Phys. Rev. A*, 74(3):030303(R), 2006.
- [43] O. V. Marchukov, E. H. Eriksen, J. M. Midtgaard, A. A. S. Kalae, D. V. Fedorov, A. S. Jensen, and N. T. Zinner. Computation of local exchange coefficients in strongly interacting one-dimensional few-body systems: local density approximation and exact results. *Eur. Phys. J. D*, 70:32, 2016.
- [44] G. De Chiara, D. Rossini, S. Montangero, and R. Fazio. From perfect to fractal transmission in spin chains. *Phys. Rev. A*, 72(1):012323, 2005.
- [45] D. Petrosyan, G. M. Nikolopoulos and P. Lambropoulos. State transfer in static and dynamic spin chains with disorder. *Phys. Rev. A*, 81(4):042307, 2010.
- [46] A. Zwick, G. A. Alvarez, J. Stolze, and O. Osenda. Robustness of spin-coupling distributions for perfect quantum state transfer. *Phys. Rev. A*, 84(2):022311, 2011.
- [47] G. M. Nikolopoulos. Statistics of a quantum-state-transfer Hamiltonian in the presence of disorder. *Phys. Rev. A*, 87(4):042311, 2013.
- [48] R. B. Diener, G. A. Georgakis, J. Zhong, M. Raizen, and Q. Niu. Transition between extended and localized states in a one-dimensional incommensurate optical lattice. *Phys. Rev. A*, 64(3):033416, 2001.